

Simple nonlinear static analysis of steel portal frame with pitched roof exposed to fire

Panagis G. Papadopoulos[†], Anastassia K. Papadopoulou[‡] and
Kyriakos K. Papaioannou^{‡†}

Department of Civil Engineering, Aristotle University of Thessaloniki, 540 06 Thessaloniki, Greece

(Received August 22, 2006, Accepted February 26, 2008)

Abstract. Plane steel portal frames, with pitched roof, exposed to fire, are examined. First, a determinate frame is analysed by hand. For flexible columns and shallow roof, snap-through occurs before plastic hinges mechanism is formed. An indeterminate frame with shorter columns and taller roof is also analysed by hand. Then, the same frame is simulated by a truss and a nonlinear static analysis is performed by use of a short computer program. The results of computer analysis by use of truss model are compared with those of analysis by hand and a satisfactory approximation between them is observed.

Keywords: steel portal frame; pitched roof; fire; snap-through; plastic hinges; truss model.

1. Introduction

A fire, occurring in a multi-bay, multi-storey frame, is usually confined in one compartment only, thus a local collapse is possible. Whereas, in a portal frame exposed to fire, a global collapse may happen, as a portal frame consists of one compartment only. This is a reason, for which the fire analysis of portal frames has attracted a particular interest (Papadopoulos and Mathiopoulou 2005, Wong 2001).

In a portal frame with pitched roof, if the beams are flexible and the roof shallow, a snap-through of roof apex is possible. The circumstances, under which a snap-through occurs in such a frame, are investigated in the literature (Scholz 1991, 1988). Recently, for the relevant problem of large deflections of plane frames, a simple formulation has been proposed based on position description (Coda and Greco 2004). The same concept is also used in the present work.

Aim of present work is to investigate the behavior of plane steel portal frames with pitched roof, exposed to fire. Wherever this is possible, simple analyses, by a hand calculator, are performed. For a more accurate nonlinear analysis of a frame, the Finite Element Method can be used. However, the usual finite elements have complicated stiffness matrices and present particular difficulties in handling nonlinear problems (Argyris 1978, 1981, 1984).

A bar of a truss is the finite element with the simplest stiffness matrix. A truss model can be used

[†] Assistant Professor, Corresponding author, E-mail: panaggpapad@yahoo.gr

[‡] Ph.D., E-mail: nat@civil.auth.gr

^{‡†} Professor, E-mail: kirpap@civil.auth.gr

as an alternative of the usual finite elements discretizations (Absi 1978, Fraternali *et al.* 2002, Papadopoulos and Mathiopoulou 2005, Papadopoulos and Karayannis 1988, Papadopoulos and Xenidis 1999, Schlaich and Schäfer 1991) and can, in a simple way, describe material nonlinearities by the nonlinear uniaxial stress-strain laws of the bars and geometric nonlinearities by writing the equilibrium conditions with respect to the deformed structure within each step of an incremental loading procedure. The truss models have been proved reliable by comparison of their results to relevant published experimental data (Papadopoulos and Karayannis 1988) and to Codes requirements (Papadopoulos and Xenidis 1999).

In the present work, for plane portal frames with pitched roof, subject to fire, a nonlinear static analysis is performed, first by a hand calculator. Then, for more accuracy, a frame is simulated by a truss and analysed by a short computer program. The corresponding results of two above analyses are compared to each other.

2. Determinate frame analysed by hand

2.1 Given data

The plane determinate symmetric steel portal frame of Fig. 1(a), with a pitched roof and a vertical load at the apex, is considered. Fig. 1(b) shows the shape and dimensions of the beam cross-section. A grade S355 steel is used as a structural material, which, for room temperature $T = 20^\circ\text{C}$, exhibits

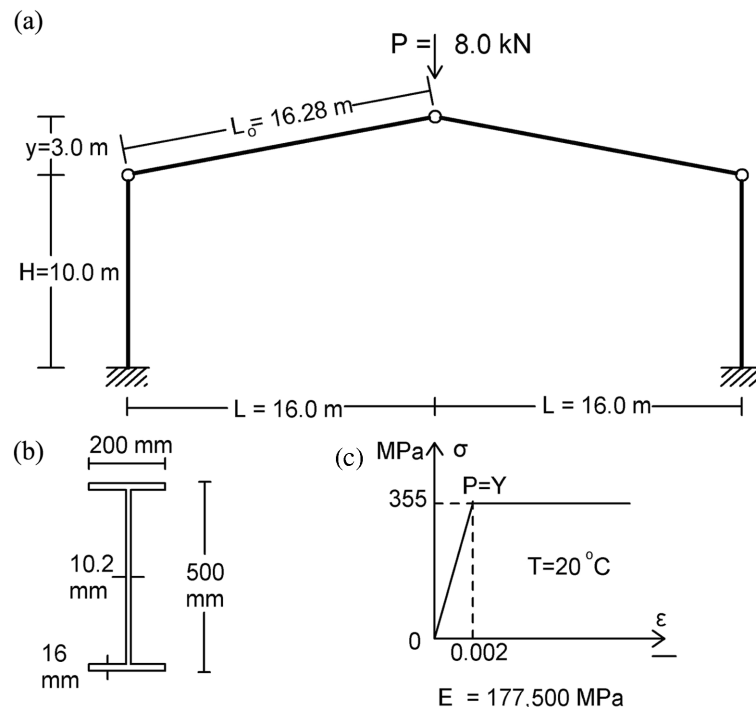


Fig. 1 Input data for a determinate portal frame. (a) Geometry and loading of the frame, (b) Cross-section, (c) Primary stress-strain curve of grade S355 steel for 20°C

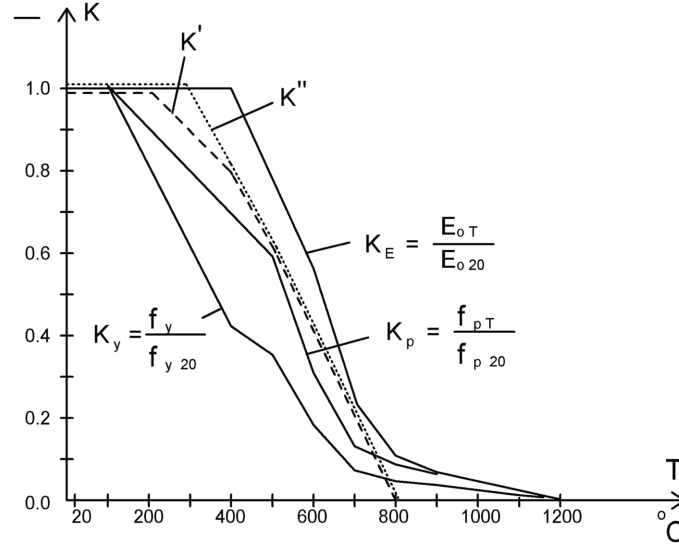


Fig. 2 Reduction factors K_Y , K_E , K_P with respect to temperature T , for the yield strength f_y of steel, the initial elasticity modulus E_o and the proportionality limit f_p , respectively, according to Eurocode 3 (1995). Proposed reduction factor K' (common for f_y , E_o , f_p) of present work for computer analysis (---) and K'' (common for f_y , E_o , f_p) for hand calculation (.....)

a bilinear elastic-perfectly plastic primary stress-strain σ - ε curve with yield strength $f_{y20} = f_{p20} = 355$ MPa and yield strain $\varepsilon_{y20} = \varepsilon_{p20} = 0.002$, as shown in Fig. 1(c).

The thermal expansion of steel is given by the formula

$$\Delta \ell = \alpha_T (T - 20^\circ\text{C})\ell \quad (1)$$

where ℓ undeformed length at temperature 20°C and the coefficient is $\alpha_T = 1.4 \times 10^{-5}/^\circ\text{C}$.

By starting from room temperature 20°C , a gradual increase of structure's temperature T is considered, with a step $\Delta T = 10^\circ\text{C}$, up to a value 800°C .

For a gradual increase of temperature T from 20°C and 100°C up to 1200°C , with a step $\Delta T = 100^\circ\text{C}$, reduction factors are suggested by Eurocode 3 (1995), for the yield strength f_{yT} , the initial elasticity modulus E_{oT} and the proportionality limit f_{pT} , as shown in Fig. 2. For intermediate values of the steel temperature, linear interpolation may be used.

For every set of values of the three parameters f_y , E_o , f_p , for a specific value of temperature T , the corresponding stress-strain σ - ε curve can be drawn, as determined by Eurocode 3 (1995) (see Fig. 3a).

For the strain range $\varepsilon_p < \varepsilon < \varepsilon_y = 0.020$, the Eurocode 3 (1995) suggests a 2nd order ellipse as a fitting stress-strain σ - ε curve, which passes through the points P and Y and has a tangent at the point P with inclination $\text{tga} = E_o$ and a horizontal tangent at the point Y .

The above 2nd order elliptical fitting σ - ε curve is expressed in Eurocode 3 (1995) by quite complicated formulas. Here, an alternative fitting σ - ε curve is proposed, in the strain range $\varepsilon_p < \varepsilon < \varepsilon_y = 0.020$, which is a 2nd order parabola, passing through the points P and Y and having a horizontal tangent at Y , and is expressed by the formula

$$\sigma = f_y - \frac{(f_y - f_p)}{(0.020 - \varepsilon_p)^2} (0.020 - \varepsilon)^2 \quad (2)$$

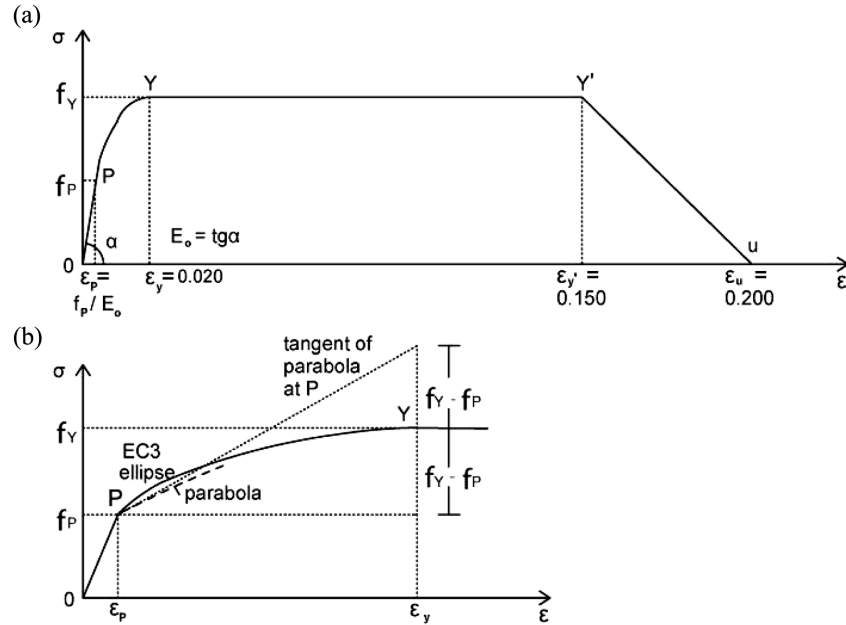


Fig. 3 (a) Primary stress-strain σ - ε curve of steel as determined by the three parameters: yield strength f_y , elasticity modulus E_o , proportionality limit f_p (for a specific temperature T), according to Eurocode 3 (1995), (b) The same σ - ε curve in the region of small strains up to $\varepsilon_y = 0.020$, with five times larger ε scale, in order to demonstrate the fitting curve between the points P and Y

where the tangent elasticity modulus is

$$E_t = d\sigma/d\varepsilon = + \frac{2(f_y - f_p)}{(0.020 - \varepsilon_p)^2} (0.020 - \varepsilon) \quad (3)$$

The above proposed parabolic fitting σ - ε curve, described by Eqs. (2), (3), is much simpler than the elliptical σ - ε curve suggested by Eurocode 3 (1995). However, the latter is smoother at point P , as shown in Fig. 3(b).

By the above prescriptions of Eurocode 3 (1995), the diagram of Fig. 4 is obtained, with the primary stress-strain σ - ε curve of grade S355 steel, for temperature T varying from 20°, 100°C up to 800°C, with a step $\Delta T = 100^\circ\text{C}$, in the strain region $0 \leq \varepsilon \leq \varepsilon_y = 0.020$. After some trials and errors, these stress-strain σ - ε curves of the diagram of Fig. 4 are approximated by simplified bilinear elastic-perfectly plastic primary stress-strain σ - ε curves, as recommended in the literature (Bruneau *et al.* 1997) (sections 2.7.2, 2.7.3, pages 45-49), which are shown in Fig. 4.

The above set of simplified bilinear elastic-perfectly plastic stress-strain σ - ε curves, which approximate the set of primary σ - ε curves of grade S355 steel suggested by Eurocode 3 (1995), corresponds to a quadrilinear reduction factor K' , common for f_y and E_o , where $f_p = f_y$ is assumed, too. This K' variation is shown in Fig. 2 by interrupted lines and is expressed by the simple formulas

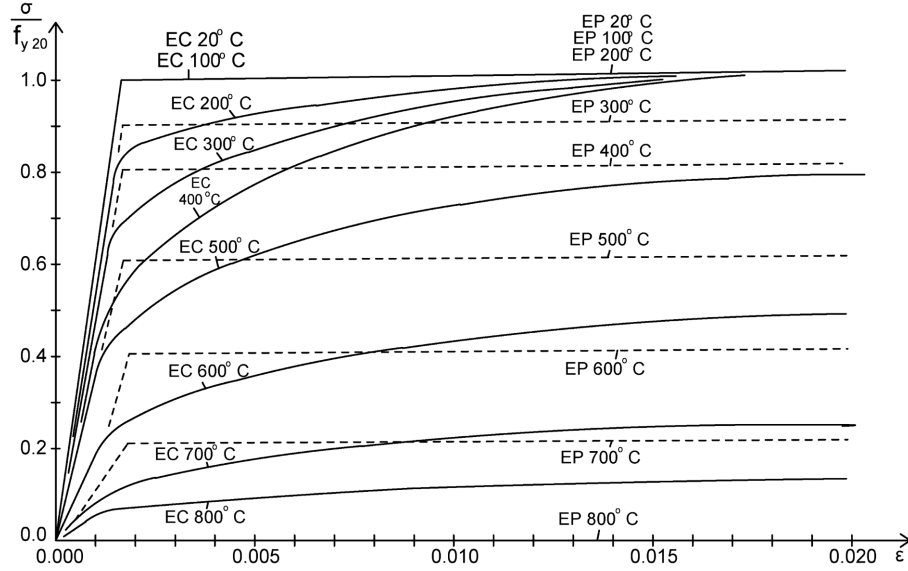


Fig. 4 Primary stress-strain σ - ε curves of grade S355 steel (strain-hardening not included), as suggested by Eurocode 3 (1995), for temperatures T starting from 20°C, 100°C and then ranging up to 800°C, with a step $\Delta T = 100^\circ\text{C}$, compared with the adopted, in the present work, corresponding elastic-perfectly plastic σ - ε curves.

Notation: EC – Eurocode, EP – elastic plastic

$$\left. \begin{aligned} 20^\circ\text{C} \leq T \leq 200^\circ\text{C} &\rightarrow K' = 1.0 \\ 200^\circ\text{C} \leq T \leq 400^\circ\text{C} &\rightarrow K' = 1.0 - 0.2 \frac{T-200}{200} \\ 400^\circ\text{C} \leq T \leq 800^\circ\text{C} &\rightarrow K' = 0.8 \left(1.0 - \frac{T-400}{400} \right) \\ 800^\circ\text{C} \leq T &\rightarrow K' = 0.0 \end{aligned} \right\} \quad (4)$$

For a further simplified hand calculation, a trilinear reduction factor K'' can be used, which is again common for f_y and E_o , where also $f_p = f_y$. This is shown in Fig. 2, by dotted lines, and is expressed by the formulas

$$\left. \begin{aligned} 20^\circ\text{C} \leq T \leq 300^\circ\text{C} &\rightarrow K'' = 1.0 \\ 300^\circ\text{C} \leq T \leq 800^\circ\text{C} &\rightarrow K'' = 1.0 - \frac{T-300}{500} \\ 800^\circ\text{C} \leq T &\rightarrow K'' = 0.0 \end{aligned} \right\} \quad (5)$$

2.2 Snap – through analysis

The geometric non-linearity is taken into account by using the concept of position for the apex, not the concept of displacement (Coda and Greco 2004). The position of the apex is defined by its ordinate y above the head of column, as shown in Fig. 5(a), in the half of the symmetric frame.

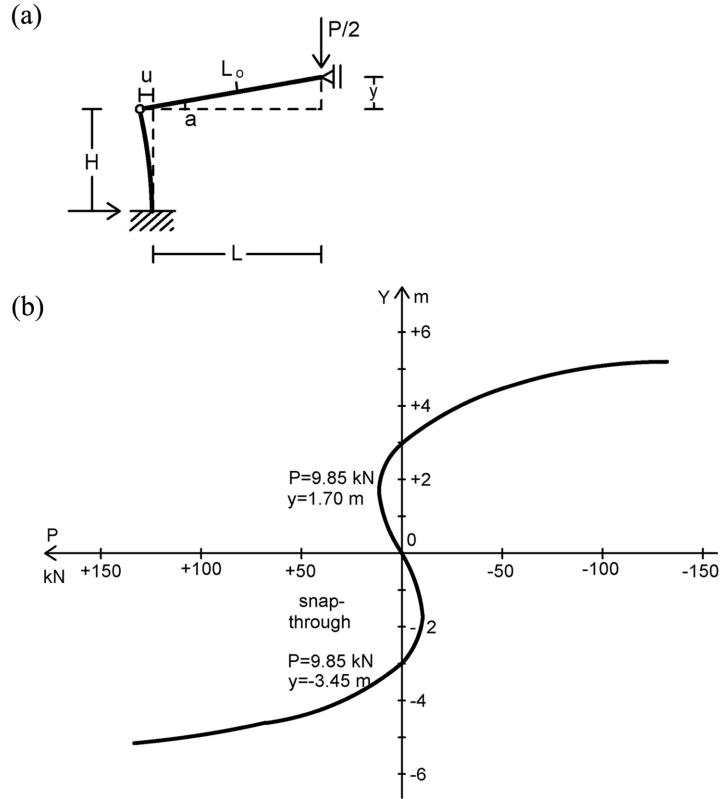


Fig. 5 (a) Position description of the half of the determinate frame, (b) Variation of the load P with respect to the apex ordinate y for $T = 20^\circ\text{C}$

For a given value of y , we can write the accurate nonlinear geometric equation, according to Pythagoras theorem

$$y^2 + (L + u)^2 = L_o^2, \quad \text{or} \\ y^2 + (16.0 + u)^2 = 16.0^2 + 3.0^2 = 265.0 \quad (6)$$

where u horizontal displacement of eave, and the reasonable assumption of constant length L_o of the rafter is adopted. From the above equation, we can easily, for a given y , find the corresponding u . The inertia moment of the beam cross-section is (Fig. 1(b))

$$J = 2 \times 1.6 \times 20 \times 24.2^2 + 1.02 \times 46.8^3/12 + 2 \times 20 \times 1.6^3/12 = 46208 \text{ cm}^4 \quad (7)$$

Thus, the lateral stiffness of the column is

$$k = \frac{3EJ}{H^3} = \frac{3 \times 17.750 \times 46208}{1000^3} = 2.4606 \text{ kN/cm} \quad (8)$$

The horizontal thrust of the column is $F_x = ku$, the inclination of the rafter $\text{tga} = y/(L + u)$ and the corresponding load at the apex $P = 2F_x \text{ tga}$. For values of y ranging from $+6.0$ m up to -6.0 m (with a step $\Delta y = 0.1$ m), by applying the above equations, the diagram of Fig. 5(b) has been drawn, which shows the variation of the load P at the apex with respect to the ordinate y of the

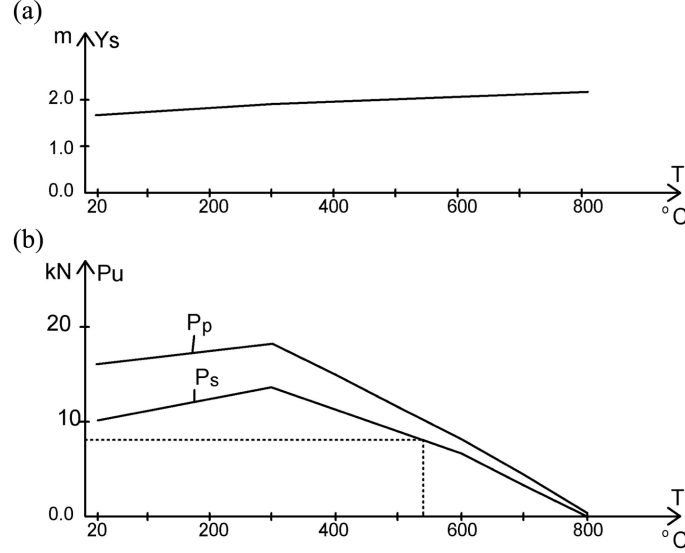


Fig. 6 Variations with respect to temperature T of: (a) The apex ordinate y_s at which snap-through occurs, (b) The snap-through critical load P_s , as well as the ultimate plastic load P_p

apex, for room temperature 20°C .

We observe in Fig. 5(b) that, for a vertical load $P = 9.851$ kN, directing downwards, for a roof ordinate $y = +1.70$ m, a snap-through of the apex occurs, which suddenly jumps to a new position $y = -3.45$ m.

All the above happen for a room temperature $T = 20^{\circ}\text{C}$. For an increase of temperature to $T = 300^{\circ}\text{C}$, the rafter expands to $1.0042L_o$, thus the unloaded roof height increases to $y = 3.3512$ m $>$ 3.0 m. By following the previous procedure, we find that the critical snap-through load increases now to $P_s = 13.63$ kN, for a roof height $y = 1.95$ m. That is, for $T = 300^{\circ}\text{C}$, the frame is strengthened against snap-through. However, for further increase of temperature, with values $T > 300^{\circ}\text{C}$, the reduction of Young modulus E leads to a reduction of column lateral stiffness, resulting to a reduction of the critical snap-through load P_s , as well.

For values of temperature T ranging from 20°C up to 800°C , the critical snap-through loads P_s and the corresponding roof heights y_s have been found and the diagrams of Fig. 6 have been drawn showing the variations $P_s - T$ and $y_s - T$.

2.3 Limit plastic analysis

In Fig. 7(a), we calculate the ultimate plastic bending moment of the beam cross-section, for $T = 20^{\circ}\text{C}$, which is $M_p = 748.1$ kNm. As M_p depends on the yield stress σ_y of steel, it remains constant up to 300°C and then linearly decreases to zero for 800°C . In Fig. 7(b), the plastic hinge collapse mechanism of the frame is presented, for which we write the virtual work principle and find the ultimate plastic load P_p

$$\frac{P}{2} \nu = M_p \vartheta = M_p \frac{u}{H} = M_p \frac{y}{LH} \nu \rightarrow P_p = 2M_p \frac{y}{LH} \quad (9)$$

In order to take into account the geometric nonlinearity, because the apex ordinate y varies

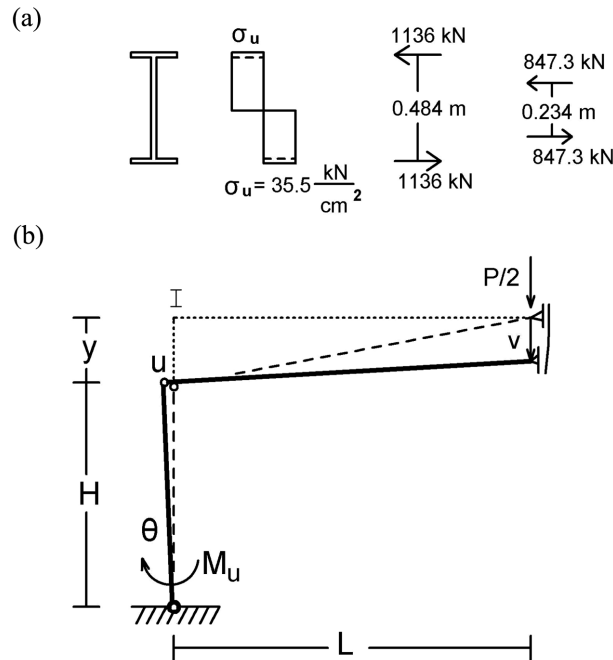


Fig. 7 (a) Ultimate plastic bending moment of beam cross-section for $T = 20^\circ\text{C}$, (b) Plastic hinge collapse mechanism of the determinate frame

significantly with the load P , we use, in the above Eq. (9), the minimum possible y for which snap-through occurs, which has been found in the previous section 2.2, Fig. 6(a), with respect to the temperature T . In this way, the plastic limit analysis becomes more realistic and, at same time, lies within the side of safety (Horne 1985).

We observe in Fig. 6(b) that, in the specific frame under consideration, for every value of temperature T , the ultimate plastic load P_p is larger than the corresponding critical snap-through load P_s . That is, the snap-through always happens before the plastic hinge collapse mechanism is formed. Thus, the snap-through determines the load that the frame can receive, and we find in Fig. 6 that, for the given external load $P = 8.0$ kN, the snap-through happens for a temperature $T \approx 540^\circ\text{C}$.

3. Indeterminate frame

3.1 Given data

The indeterminate portal frame of Fig. 8 is now examined. The columns are shorter, thus stiffer and the roof taller than in previous example. Two vertical loads $P = 80$ kN are applied at the middles of the rafters. All the other given data are the same as in the first application.

Obviously, this second frame is stronger than the first one, that is it can receive heavier loads. Also, it will be shown that this frame finally fails by formation of a plastic collapse mechanism, not by a snap-through effect.

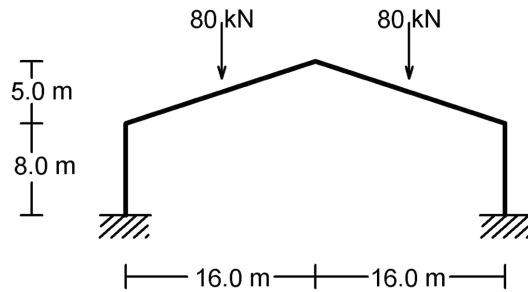


Fig. 8 Input data for an indeterminate portal frame

3.2 Static loading and thermal expansion analysis by hand

For $T = 20^{\circ}\text{C}$, the linear analysis of the frame is performed, for the static loading, by a hand calculator. The results are shown in Fig. 9(a). As the Young modulus E varies with T , it can be shown that the stresses of the frame due to static loading remain constant, whereas the deformations due to static loading are constant up to 300°C and then, for $T > 300^{\circ}\text{C}$, they increase being multiplied by the ratio $500/(800 - T)$.

For $T = 300^{\circ}\text{C}$, the linear analysis of the frame is performed by hand, for thermal expansion only, without static loading. The results are shown in Fig. 9(b).

It can be shown that the thermal deformations are proportional to the temperature T , whereas the thermal stresses, up to $T = 300^{\circ}\text{C}$, are proportional to T and then, for $T > 300^{\circ}\text{C}$, they vary by the ratio $10^{-4}/15 T (800 - T)$, having as reference state that for 300°C , and they present a maximum value for $T = 400^{\circ}\text{C}$, for which this ratio becomes 1.067.

For T ranging from 20°C up to 800°C , we find the vertical apex displacement, due to static loads on one hand and to thermal expansion to the other, as well as the total displacement ν . The results

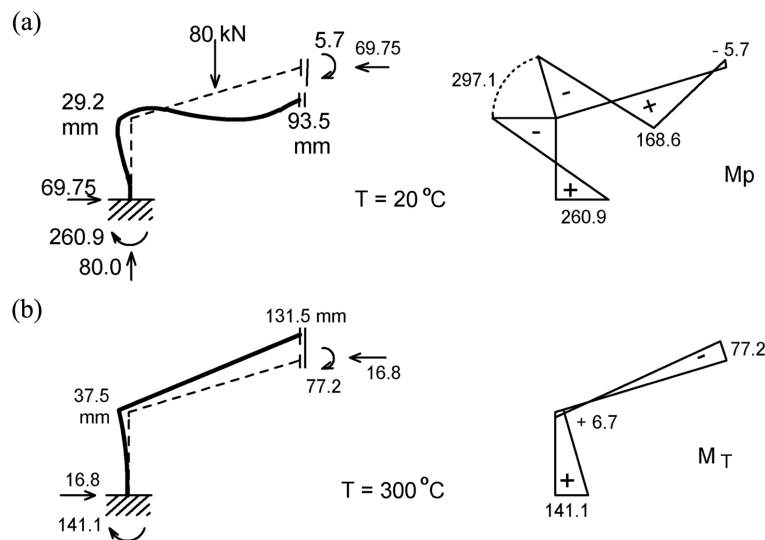


Fig. 9 Linear analysis of the indeterminate frame. (a) Static loading for $T = 20^{\circ}\text{C}$, (b) Thermal expansion for $T = 300^{\circ}\text{C}$

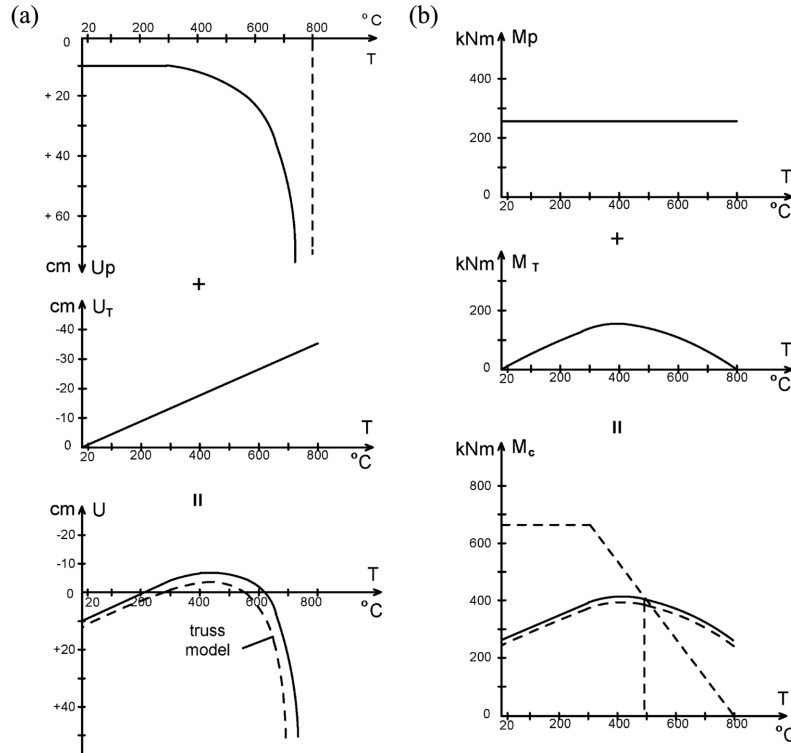


Fig. 10 Variation with respect to temperature T of: (a) Vertical displacement v of the apex, (b) Bending moment M_c at the base of column. Both due first to static loading, then to thermal expansion and total values

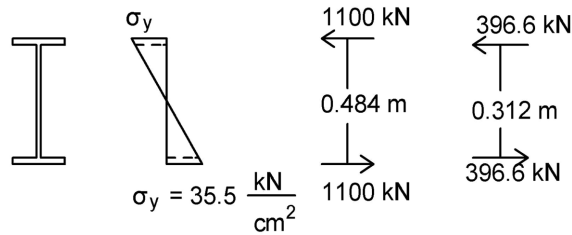


Fig. 11 Bending moment M_y of beam cross-section when yielding starts at the outer surfaces of flanges, for room temperature $T = 20^\circ\text{C}$

are shown in Fig. 10(a).

Also, for T ranging from 20°C up to 800°C , we find the bending moment at the base of column, due to static loads on one hand and to thermal expansion on the other hand, as well as the total moment M_c , as shown in Fig. 10(b).

Fig. 11 shows a simple computation of the bending moment M of the beam cross-section when yielding starts at the outer surfaces of the flanges for 20°C . This is

$$\begin{aligned}
 M_y &= 1100 \text{ kN} \times 0.484 \text{ m} + 396.6 \text{ kN} \times 0.312 \text{ m} = \\
 &= 532.4 \text{ kNm} + 123.7 \text{ kNm} = 656.1 \text{ kNm}
 \end{aligned}
 \tag{10}$$

This yield bending moment M_y of the section remains constant up to $T = 300^\circ\text{C}$ and then linearly decreases up to zero for $T = 800^\circ\text{C}$. In Fig. 10(b), the bilinear curve representing the variation of M_y with respect to T intersects the curve representing the variation of the maximum bending moment M_c of the frame, at the base of the column, with respect to T , at a point where $T = 492.8^\circ\text{C}$ and $M_c = M_y = 403.2 \text{ kNm}$. That is, the linear static analysis strictly holds up to the temperature $T = 492.8^\circ\text{C}$. For higher temperatures, some deviations from linearity start to appear.

3.3 Limit plastic analysis by hand

We consider a collapse mechanism of the frame with three plastic hinges, at the sections where the bending moments with maximum absolute values appear, as shown in Fig. 12(a) for $T = 20^\circ\text{C}$. We write the virtual work principle for this collapse mechanism

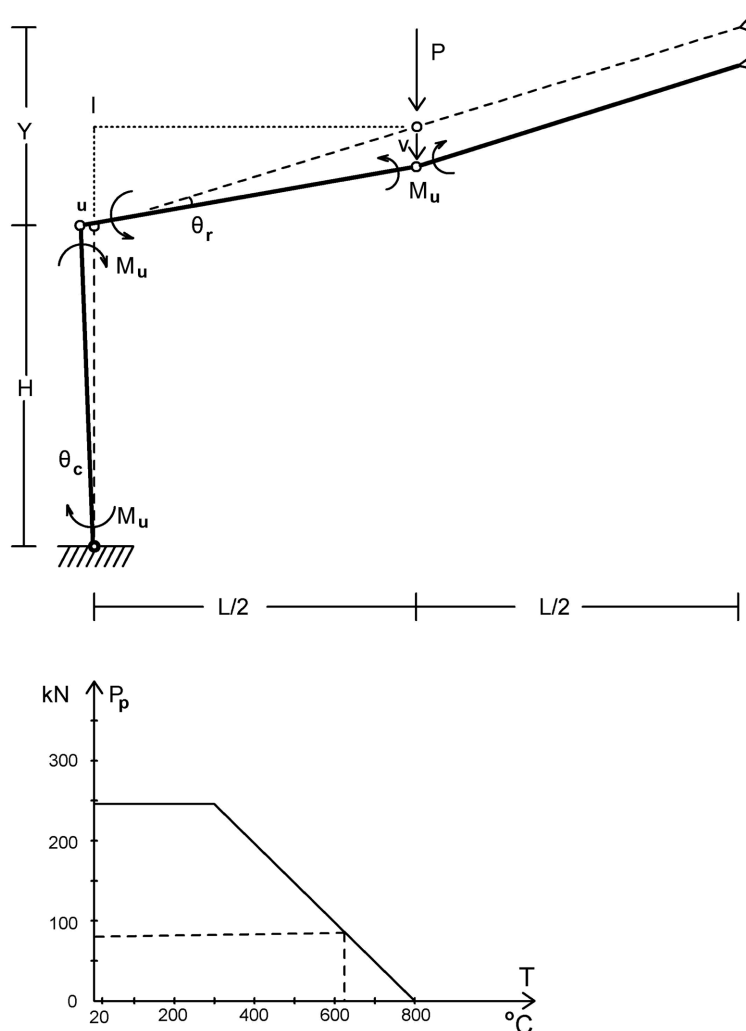


Fig. 12 (a) Plastic hinges collapse mechanism of the indeterminate frame, (b) Variation of the ultimate plastic load P_p with the temperature T

$$\begin{aligned}
P_v &= 2M_u \vartheta_r + 2M_u \vartheta_c = 2M_u \left(\frac{v}{L/2} + \frac{u}{H} \right) = 2M_u \left(\frac{2v}{L} + \frac{vu}{LH} \right) \\
\rightarrow P_p &= \frac{2M_u}{L} \left(2.0 + \frac{v}{H} \right) = \frac{2 \times 748.1}{16.0} \left(2.0 + \frac{5.0}{8.0} \right) = 245.6 \text{ kN}
\end{aligned} \tag{11}$$

As the M_u significantly varies with T , whereas v , H slightly vary, we determine the variation of the ultimate plastic load P with T , which is shown in Fig. 12(b). We observe that, for the external load $P = 80 \text{ kN}$, the plastic collapse mechanism is formed for $T = 625.0^\circ\text{C}$.

3.4 The proposed truss model

In order to perform a more accurate nonlinear analysis of the frame under consideration, by taking into account in detail the material nonlinearities i.e. the gradual formation of plastic hinges, and the geometric nonlinearities i.e., $N-M$ (axial force-bending moment) interaction, due to large displacements, we can use the Finite Element Method (Argyris 1978, 1981, 1984). However, the usual Finite Elements have complicated stiffness matrices and present particular difficulties in handling nonlinear problems.

A bar of a truss is the Finite Element with the simplest local stiffness matrix. And a truss model can be used as an alternative of a usual finite element discretization (Absi 1978, Fraternali *et al.* 2002, Papadopoulos and Mathiopoulou 2005, Papadopoulos and Karayannis 1988, Papadopoulos and Xenidis 1999, Schlaich and Schäfer 1991). A truss model can simply take into account material nonlinearities by the nonlinear uniaxial stress-strain laws of the bars and geometric nonlinearities by writing the equilibrium conditions with respect to the deformed structure and updating the stiffness matrix of the truss within each step of an incremental loading procedure.

Numerical results by truss models have been compared with published experimental data (Papadopoulos and Karayannis 1988) and Codes requirements (Papadopoulos and Xenidis 1999) and a satisfactory approximation between them has been observed.

The local stiffness matrix of a bar, in 2D, is written

$$\mathbf{\kappa}_\ell = \begin{pmatrix} \kappa_o & -\kappa_o \\ -\kappa_o & \kappa_o \end{pmatrix} \tag{12}$$

where

$$\mathbf{\kappa}_o = \mathbf{\kappa}_e + \mathbf{\kappa}_g = \frac{EA}{\ell_o} \bar{c} \bar{c}^t + \frac{N}{\ell} \mathbf{I}_2 = \frac{E}{\ell_o} \begin{pmatrix} c_x^2 & c_x c_y \\ c_x c_y & c_y^2 \end{pmatrix} + \frac{N}{\ell} \begin{pmatrix} 1 & 0 \\ 0 & 1 \end{pmatrix} \tag{13}$$

and $\mathbf{\kappa}_e$ elastic stiffness, $\mathbf{\kappa}_g$ geometric stiffness, E elasticity modulus, A cross-section area, ℓ_o undeformed length of the bar, $\bar{c} = \{c_x \ c_y\}$ direction cosines of bar axis, N axial force, present length of the bar.

The global stiffness matrix of the bar is written

$$\mathbf{K}_G = \mathbf{B} \text{diag} (\mathbf{\kappa}_o) \mathbf{B}^t \quad i = 1 \dots n_b, \tag{14}$$

where $\mathbf{B} = (B_{i\kappa})$, $i = 1 \dots n_n$, $\kappa = 1 \dots n_b$, the Boolean linkage matrix of the truss, n_n number of nodes, n_b number of bars, $B_{i\kappa} = -1$ if node i is left end of bar κ , $B_{i\kappa} = +1$ if node i is right end of bar κ and $B_{i\kappa} = 0$ if there is no connection between node i and bar κ .

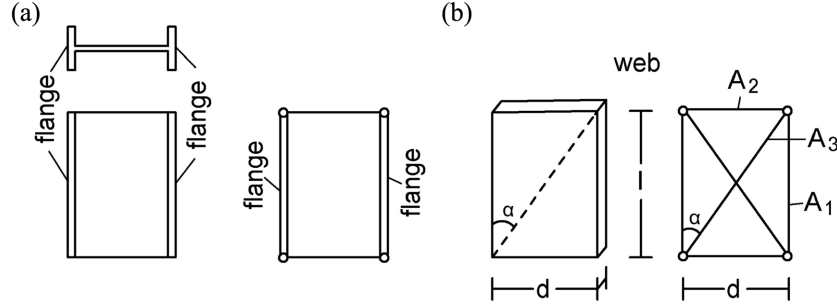


Fig. 13 Simulation of a steel beam element, with double – tau section, by a plane truss element

If we have to simulate a usual steel beam element with a double-tau cross-section, by a rectangular plane truss element, the flanges are first, in a simple and obvious way, simulated by bars (Fig. 13(a)).

Then, by considering the correspondence between the biaxial elasticity equations of a plate element, which is the web of the steel beam element, and the nodal force-displacement equations of the rectangular plane truss element and by assuming a Poisson ratio $\nu = 1/3$, we determine the sections of bars of the truss element (Fig. 13(b)), by the following formulas

$$\left. \begin{aligned} \frac{A_3 \cos^2 \vartheta \sin \vartheta}{9/8 \times td/2} &= \frac{1}{3} \rightarrow A_3 \\ A_3 \cos^3 \vartheta + A_1 &= \frac{9}{8} \times \frac{td}{2} \rightarrow A_1 \\ A_3 \sin^3 \vartheta + A_2 &= \frac{9}{8} \times \frac{t\ell}{2} \rightarrow A_2 \end{aligned} \right\} \quad (15)$$

If the angle of the web element, in Fig. 13(b), is $\alpha < 21^\circ$, the above formulae cannot be used because negative sections A_1 result, which is inadmissible. In this case of a long web element with $\ell \gg d$ and $\alpha < 21^\circ$, the following simplified formulae can be used for the determination of bar sections of the truss element simulating the web of the beam element (Fig. 13(b))

$$\left. \begin{aligned} A_1 &= A_3 = td/4 \\ A_2 &= t\ell/2 \end{aligned} \right\} \quad (16)$$

A short, thus transparent, computer program, with only about 350 Fortran instructions, has been developed for the analysis of a plane truss model, by an incremental loading (temperature increase) procedure, by taking into account material and geometric nonlinearities.

3.5 Discretization of the frame

The column of the frame under consideration is discretized by four truss elements (Fig. 14). The rafter is discretized by eight elements. And there is one more element for the column-rafter joint. That is, there are totally $8 + 4 + 1 = 13$ elements, thus 28 nodes, which means that an algebraic system 56×56 of equilibrium equations is solved within each step of the incremental loading algorithm. There are $13 \times 5 = 65$ bars. The two nodes at the base of column have both DOFs

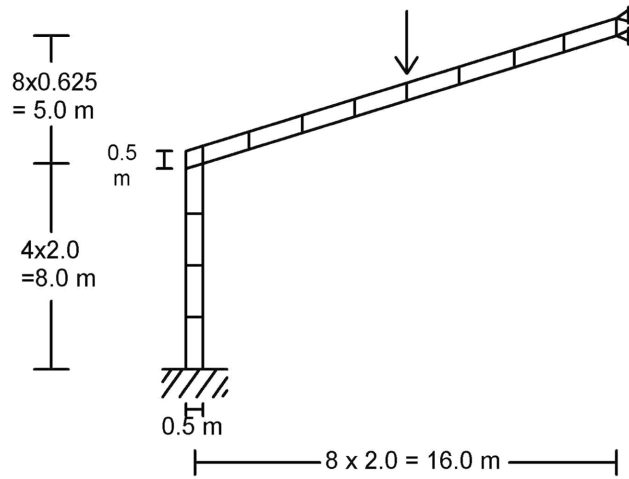


Fig. 14 Discretization of the indeterminate frame

restricted. The two nodes of rafter, at symmetry axis, have the horizontal DOFs restricted. For the determination of bar sections, all the elements are approximately considered as rectangular. The column and rafter elements are long with $l \approx 4d$ and $\alpha \approx 14^\circ < 21^\circ$ (Fig. 13(b)), thus the simplified formulae (16) are used for the determination of bar sections. Only the rafter-column joint element is short with $l \approx d$, thus $\alpha \approx 45^\circ > 21^\circ$, so here the formulae (15) are used for the determination of bar sections.

3.6 Results of truss model

The results of the analysis of the second application (indeterminate frame) by the truss model are presented in Fig. 15, for the following characteristic temperatures: (1) Room temperature $T = 20^\circ\text{C}$. (2) $T = 200^\circ\text{C}$, up to which yield stress σ_y and elasticity modulus E_o of steel are assumed constant, equal to their initial values. (3) $T = 400^\circ\text{C}$, for which σ_y , E_o are reduced to eighty percent of their initial values. (4) $T = 570^\circ\text{C}$, at which, for first time, a bar yields (a web diagonal bar at the base of column).

For every one of the above four characteristic temperatures, the deformed configuration of the frame has been drawn, with a large scale for displacements, along with the free body diagram of the frame (Fig. 15).

Fig. 16 shows the plastic collapse mechanism of the frame, which happens at a temperature $T = 610^\circ\text{C}$, close to the value $T = 625^\circ\text{C}$ found by the limit plastic calculation done by hand. However, a different failure mode is revealed by the truss model: The yielding of the column is of shear type that is the diagonals of the web yield, whereas the hand limit plastic calculation assumed the formation of a plastic hinge at the base of the column.

In Figs. 10(a,b), the variations with T of total vertical apex displacement v , and of total bending moment M_c at base of column, respectively, obtained by the truss model, are compared with the corresponding ones, obtained previously by the linear hand calculation, and a satisfactory approximation between them is observed.

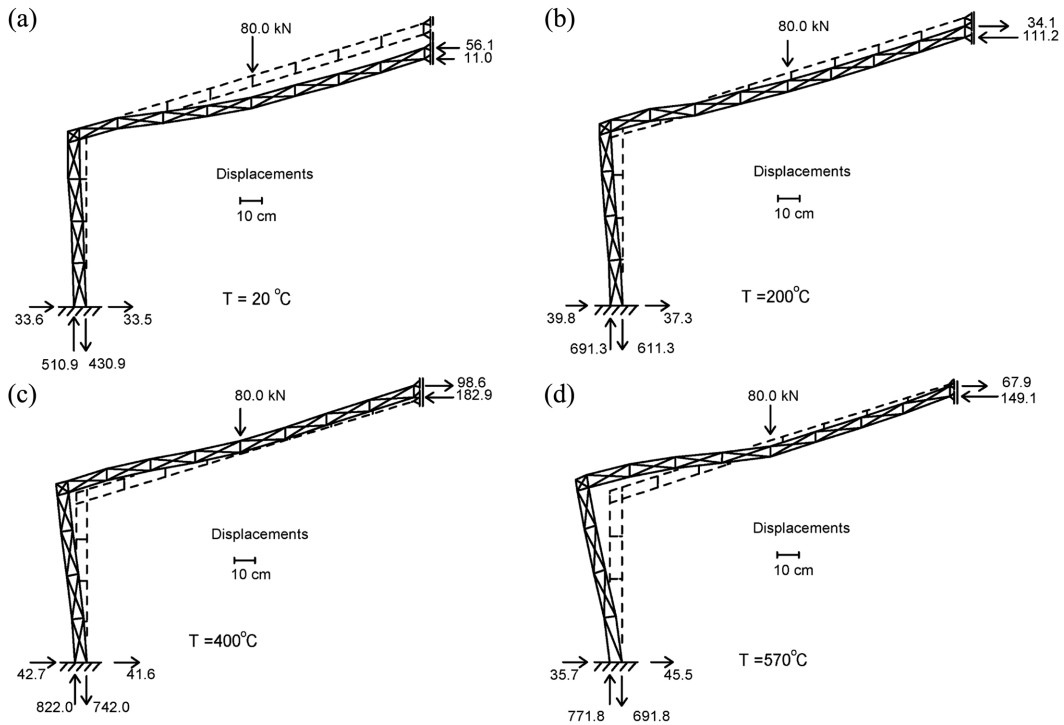


Fig. 15 Results (deformed configuration and free body diagram) of the truss model of the indeterminate frame, for characteristic temperatures: (a) Room temperature $T = 20^{\circ}\text{C}$, (b) $T = 200^{\circ}\text{C}$ up to which yield strength f_y and elasticity modulus E_o remain constant, (c) $T = 400^{\circ}\text{C}$ at which the σ_y , E_o are reduced to the 0.8 of their initial values, (d) $T = 570^{\circ}\text{C}$ when, for first time, a bar yields (web diagonal at the base of column)

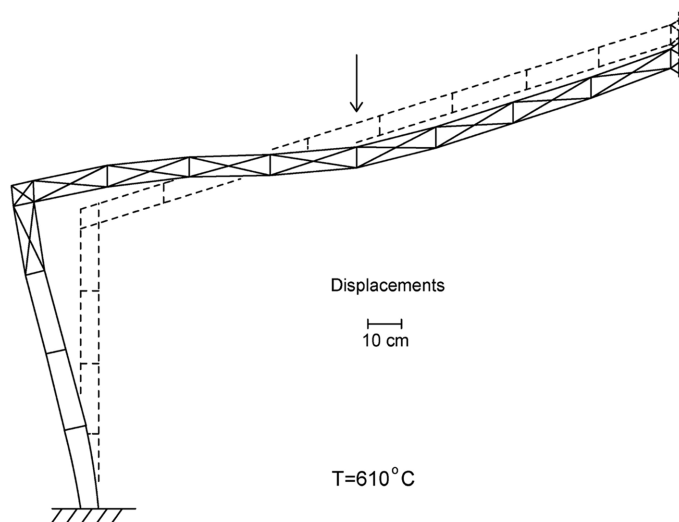


Fig. 16 Plastic collapse mechanism of the indeterminate frame, revealed by the truss model, due to shear yield at the column web, for temperature $T = 610^{\circ}\text{C}$

4. Conclusions

1. In a determinate portal frame with pitched roof, a simple analysis by hand can be performed, in order to investigate the snap-through effect.

2. If the columns of the frame are flexible and the pitched roof shallow, snap-through may occur before the formation of a plastic collapse mechanism.

3. In a simplified linear analysis of an indeterminate frame for static loading only, it is observed that the stresses remain constant for any temperature T , whereas the deformations are constant up to $T = 300^\circ\text{C}$ and then, for $T > 300^\circ\text{C}$, as Young modulus decreases, they increase by the ratio $500/(800 - T)$.

4. In a simplified linear analysis of an indeterminate frame for thermal expansion only, it is observed that the deformations increase proportionally with the temperature T , whereas the stresses, for $T \leq 300^\circ\text{C}$, increase proportionally with T , and then, for $T > 300^\circ\text{C}$, they vary by the ratio $(10^{-4}/15) T(800 - T)$, which takes a maximum value 1.067 for $T = 400^\circ\text{C}$.

5. For an accurate nonlinear analysis, a frame can be simulated by a truss model. A bar of a truss is the finite element with the simplest local stiffness matrix. And a truss model can simply take into account material nonlinearities by the nonlinear uniaxial stress-strain laws of the bars and geometric nonlinearities by writing the equilibrium conditions with respect to the deformed structure and by updating the stiffness matrix of the truss within each step of an incremental loading (temperature increase) procedure.

6. Numerical results for a steel frame exposed to fire, obtained by a truss model, are found in a satisfactory approximation with corresponding results obtained by a linear hand calculation, as regards to deformations and reactions for various values of temperature, as well as the temperature of the final plastic collapse mechanism of the frame. However, a different failure mode is revealed by the truss model: A yielding of diagonals is observed in the column web, which is a shear yield. Whereas the hand limit plastic analysis assumed the formation of a plastic hinge at the base of column.

7. In the region of a primary stress-strain σ - ε curve of steel (for a specific temperature T) between the proportionality limit P and the yield point P , a 2nd order parabolic fitting σ - ε curve is proposed, in the present work, which is much simpler than the corresponding elliptical curve proposed by the Eurocode 3 (1995). However, the latter is smoother in the vicinity of proportionality limit.

References

- Absi, E. (1978), *Méthodes des Calcul Numérique en Élasticité*, Eyrolles, Paris.
- Argyris, J.H. Editor. F.E.No.Mech. (Finite Elements in Nonlinear Mechanics). International Conferences. Institute for Statics and Dynamics, University of Stuttgart, I. 1978, II. 1981, III. 1984.
- Bruneau, M., Uang, C.-M. and Whittaker, A. (1997), *Ductile Design of Steel Structures*. McGraw-Hill.
- Coda, H.B. and Greco, M.A. (2004), "A simple FEM formulation for large deflection 2D frame analysis, based on position description", *Comput. Meth. Appl. Mech. Eng.*, **193**, 3551-3557.
- Eurocode 3 (1995), *Design of Steel Structures. Part 1-2. Fire Resistance*. ENV 1993-1-2.
- Fraternali, F., Angelilo, M. and Fortunato, A. (2002), "A lumped stress method for planar elastic problems and their discrete-continuum approximation", *Int. J. Solids Struct.*, **39**, 6211-6240.
- Horne, M.R. (1985), Frame Instability and the Plastic Design of Rigid Frames, in Narayanan R., Editor. "Steel framed structures" Elsevier.

- Papadopoulos, P.G. and Mathiopoulou, A.K. (2005), "Analysis of portal steel frame exposed to fire by use of a truss model", *Proc. of 8th Int. Conf. on Advanced Computational Methods in Heat Transfer*, 495-505, Lisbon, 24-26 March.
- Papadopoulos, P.G. and Karayannis, C.G. (1988), "Seismic analysis of RC frames by network models", *Comput. Struct.*, **28**, 253-267.
- Papadopoulos, P.G. and Xenidis, H.C. (1999(II)), "A truss model with structural instability for the confinement of concrete columns", *J. Euro. Earthq. Eng.*, 57-80.
- Schlaich, J. and Schäfer, K. (1991), "Designing and detailing structural concrete using strut-and-tie models", *Struct. Eng.*, **69**, 113-125.
- Scholz, H. (1991), "Stability control of pitched roof frames by allowable member depth", *J. Constr. Steel Res.*, **18**, 253-267.
- Scholz, H. (1988), "A new solution to the snap-through of pitched roof steel frames", *J. Constr. Steel Res.*, **9**, 265-285.
- Wong, M.B. (2001), "Elastic and plastic methods for numerical modeling of steel structures subject to fire", *J. Constr. Steel Res.*, **57**, 1-14.